

Facile fabrication of graphene-based high-performance microsupercapacitors operating at high temperature of 150 °C

Viktoriia Mishukova,^a Nicolas Boulanger,^b Artem Iakunkov,^b Szymon Sollami Delekta,^a Xiaodong Zhuang,^c Alexandr Talyzin^b and Jiantong Li^{*,a}

^a *KTH Royal Institute of Technology, School of Electrical Engineering and Computer Science, Electrum 229, SE-164 40 Kista, Sweden. E-mail: jiantong@kth.se*

^b *Department of Physics, Umeå University, Umeå SE-901 87, Sweden*

^c *The Soft2D Lab, State Key Laboratory of Metal Matrix Composites, Shanghai Key Laboratory of Electrical Insulation and Thermal Ageing, School of Chemistry and Chemical Engineering, Shanghai Jiao Tong University, Shanghai, 200240 China*

Corresponding Author

*E-mail: jiantong@kth.se

Electronic Supplementary Information

Graphene ink formulation. The activated graphene ink was prepared based on the previous work,¹ mainly including the following three steps: (1) Activated reduced graphene oxide (a-rGO) was prepared through thermal activation of reduced graphene oxide (rGO, Abalonyx, Norway) by using slightly modified KOH activation procedure optimized for high surface area.¹ (2) The aqueous a-rGO dispersion was prepared through sequential mixing of the components using Mixed Mill MM400 vibrational ball milling machine (RetschVolume) equipped with an agate cell. Each mixing step was under the oscillation frequency of 30 s^{-1} for 5 minutes. First, graphene oxide (GO, Abalonyx, Norway) and nanocrystalline fumed silica (Sigma-Aldrich) were mixed with the aqueous dispersion medium. Then carbon nanotubes (CNTs, OCSiAl) were added and mixed. Finally, the a-rGO was added and mixed. The optimized component weight ratio was 10:1:1:1 (a-rGO : GO : SiO₂ : CNT). The concentration of a-rGO in the final aqueous dispersion was 20 mg/ml. (3) The sacrificial viscosifier, xanthan gum (TCI Europe), was added at the concentration of 10 mg/mL to the a-rGO aqueous dispersion and magnetically stirred at 300 rpm for 2 hours to obtain the viscous stable graphene inks, as shown in Figure S1.



Figure S1 Photograph of the final viscous stable graphene ink (upside down).

Characterization of the a-rGO. The a-rGO used in this study was from the same batch as in our previous studies of the a-rGO.^{1,2} This batch was characterized in detail using X-ray photoelectron spectroscopy (XPS), Nitrogen sorption isotherms, scanning electron microscopy (SEM), X-ray diffraction analysis (XRD), Raman spectroscopy and thermogravimetric analysis in our earlier publications.¹ Here we provide a short summary of this characterization. The precursor a-rGO material showed no diffraction peaks in XRD and low oxygen content (C/O=55 determined by comparing areas of C1s and O1s) according to XPS. Specific Surface Area (SSA) was determined using analysis of nitrogen sorption for the a-rGO sample used in this study for preparation of dispersions showing $\sim 2580\text{ m}^2/\text{g}$ by Brunauer–Emmett–Teller (BET) surface analysis and $\sim 2150\text{ m}^2/\text{g}$ using quenched solid density functional theory (QSDFT) model. The analysis of the nitrogen sorption isotherm using

QSDFT slit pore model showed almost 100% of pore volume is in pores with diameter below 4 nm. Porous structure of a-rGO was also confirmed using direct microscopic characterization using SEM and scanning transmission electron microscopy.² Hydrophobic nature of a-rGO was also confirmed using Dynamic vapor sorption method. The sample of a-rGO, similar to the one used here for preparation of electrodes, showed almost negligible BET SSA value of $\sim 8 \text{ m}^2/\text{g}$ by water sorption. However, relatively large pore volume of $0.87 \text{ cm}^3 \text{ g}^{-1}$ was measured using full isotherm which exhibits the shape that points out to condensation of water inside the pores at P/P_0 above ~ 0.7 .¹ XRD patterns of coated electrodes are mostly a sum of XRD from all components. Ball milling used for preparation of dispersions provides additional disorder. As a result, XRD of a-rGO electrodes exhibits one broad and asymmetric peak centered at ~ 5.9 degrees (d-spacing 14.98 \AA) and a small peak from graphitic $d(002)=3.35 \text{ \AA}$. Both peaks are likely to originate from mechanically deformed CNTs bundles ($d(100)=16.99 \text{ \AA}$ in the pattern of precursor CNTs). Precursor a-rGO shows only one weak XRD reflection with $d=2.08 \text{ \AA}$ (due to in-plane graphene lattice) and strong diffuse scattering at low angles. This is due to disordered structure of porous sample. The BET specific surface area was evaluated by analysis of nitrogen sorption isotherms acquired using Autosorb iQ XR analyzer by Quantachrome.

Electrolyte formulation. To prepare high-temperature gel electrolyte, 200 mg of poly(vinylidene fluoride-co-hexafluoropropylene) (PVdF-HFP) (Sigma-Aldrich Sweden AB) was dissolved in 10 mL acetone in a glass bottle at $60 \text{ }^\circ\text{C}$ under stirring for 4 hours.³ Then, 1.5 mL of ionic liquid (IL), 1-butyl-3-methylimidazolium tetrafluoroborate, (BMIM-BF₄) ($\geq 97.0\%$ (HPLC), Merck), was added into the mixture and stirred for 2 hours until the mixture became homogeneous.

Device fabrication. To make a MSC, 60 μL of formulated graphene ink was drop cast onto a 1 mm thick glass substrate (SuperFrost, VWR Collection) to form a uniform film. The glass substrate was pre-cleaned sequentially in acetone and isopropanol with the assistance of an ultrasonic bath. To dry the ink droplets and remove residual binders the graphene film underwent a two-step heating process: 30 minutes drying at $60 \text{ }^\circ\text{C}$, followed by 30 minutes annealing at $300 \text{ }^\circ\text{C}$. Next, the graphene film was patterned into interdigitated device structure by using fiber laser (Raycus, continuous wave, $\lambda = 1064 \text{ nm}$) with a beam power of 9 W. As shown in Figure 1a, each device consisted of three pairs of fingers with a finger length of 4.5 mm, a finger width of 1 mm, a finger gap of 500 μm and a total area of 0.6 cm^2 . Once patterning was finished, the structures were blown with nitrogen gas to remove any residual vaporized particles from the substrate. Then, the electrical resistance between the two electrodes was measured to make sure of their electrical separation. Finally, the electrolyte mixture (30 μL) was drop-cast onto the interdigitated electrodes to cover the active area of the device and let dry for 30 minutes.

Repeatability study. In order to study repeatability of our drop casting process, KLA-Tencor P-15 Profilome-

ter was used to characterize the thickness profile of the cast graphene ink drops. Four drops of ink (each of volume of 60 μL) were cast onto a glass substrate to form four circular films, denoted as Drops A, B, C and D, respectively. The profiles of drops was characterized after the two-step heating process following the electrode preparation procedure. As shown in Figure S2, all the drops exhibit similar profile with a thinned center.

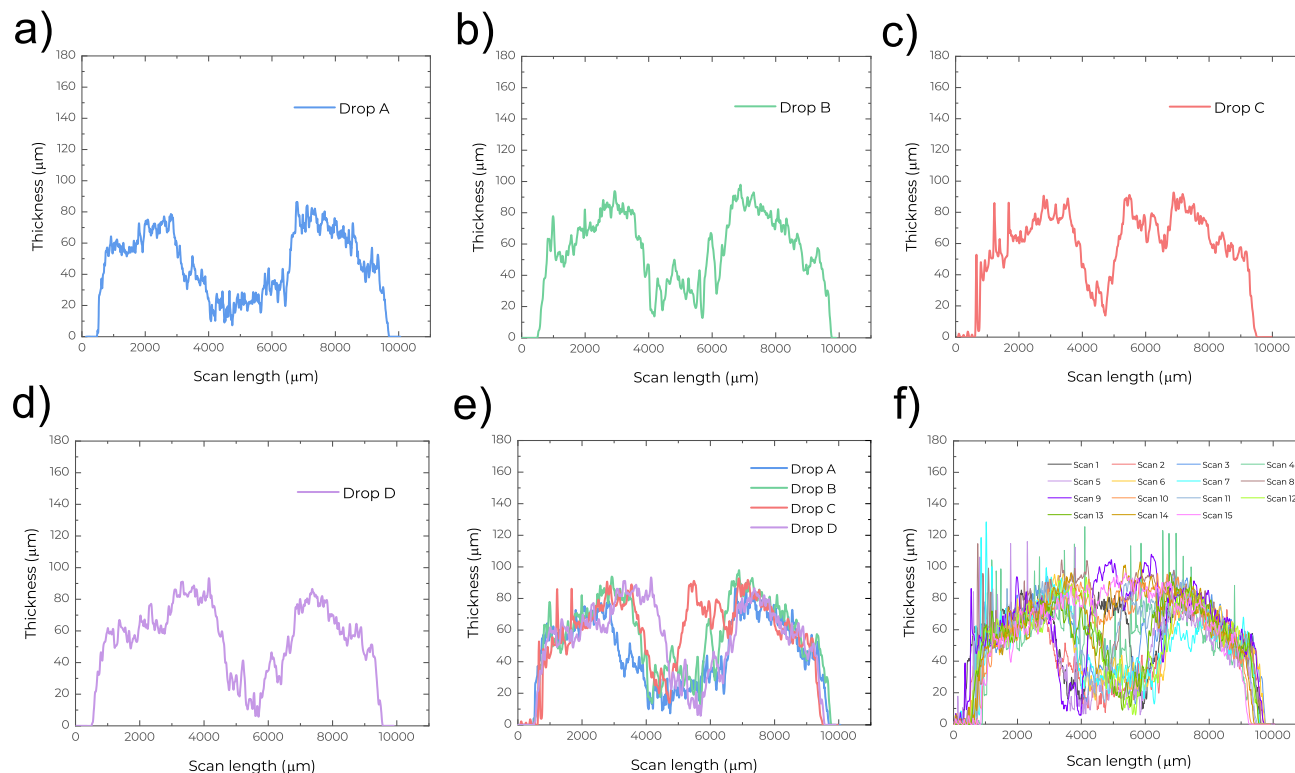


Figure S2 Profilometric analysis of the drop cast ink on glass substrate. Profilometric curves (a), (b), (c) and (d) for Drops A, B, C and D, respectively. (e) An overlapping plot of profilometric curves for all the four drops to indicate the repeatability of drop casting process. (f) An overlapping plot of 15 different scan paths on the four samples

Further analysis shows that the average thickness of the four drops varies in the range of 51 to 62 μm (Table S1) and their diameter was all around 9 mm.

Table S1 Average thickness of the drop cast ink obtained during profilometric analysis

Sample	Average thickness (μm)	Average diameter (mm)
Drop A	51.0	9.2
Drop B	57.2	9.0
Drop C	62.1	8.9
Drop D	59.6	9.2

Patterned electrodes were studied using profilometric analysis as well (Figure S3). After the profilometric analysis of the cast Drops A, B, C were laser scribed to obtain interdigitated electrodes (each with three pairs of fingers), denoted as IDEs A, B and C, respectively. Each sample with patterned interdigitated electrodes

was scanned two times in different locations and across the 6 fingers of the device. The average calculated thicknesses of electrodes are presented in the Table S2 and are in the range of 36 to 45 μm .

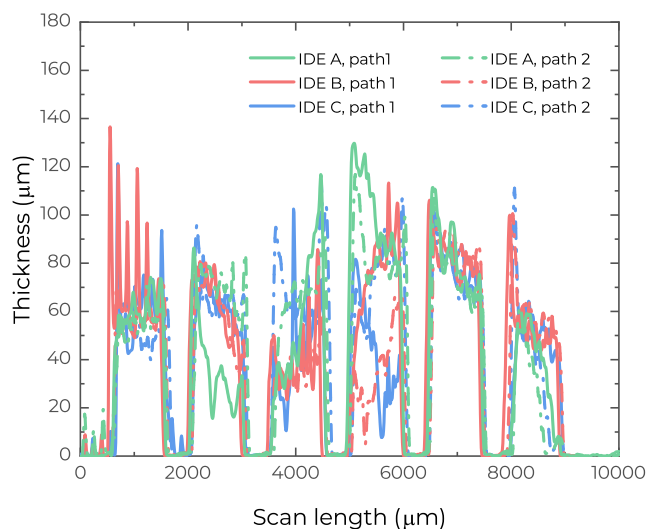


Figure S3 Profiles at different scan positions of IDEs A, B and C

Table S2 Average electrode thickness obtained from profilometric analysis

Sample name	Average thickness (μm)
IDE A, path 1	40.8
IDE A, path 2	39.7
IDE B, path 1	38.6
IDE B, path 2	36.5
IDE C, path 1	45.1
IDE C, path 2	39.8

To confirm repeatability of the device fabrication we have fabricated three MCSs as Devices I, II and III, respectively. Figure S4 indicated their electrochemical performance (cyclic voltammetry). It was shown that the repeatability of drop casting and laser scribing manifests in the performance of our MSCs with a small device-to-device variation. The average capacitance among the three devices was $9.4 \pm 2.3 \text{ mF/cm}^2$.

Device characterization. Sheet resistance measurements were performed on the 4-point probe station Four Dimensions, Model 280. Cyclic voltammetry, galvanostatic charge-discharge, electrochemical impedance spectroscopy analyses were performed using Gamry Interface 1010E potentiostat (Gamry Instruments Inc., Warminster PA, USA) in a combination with Signatone S-1060R 4" Hot Chuck probe station with the 1 $^{\circ}\text{C}$ accuracy.

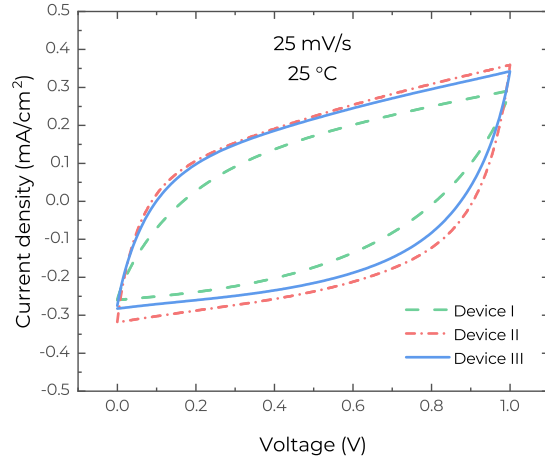


Figure S4 CV curves obtained at a scan rate of 25 mV/s for different MSCs at 25 °C.

The areal capacitance was extracted from cyclic voltammetry curves using Equation S1:

$$C_{A,CV} = \frac{\int_0^{\Delta V} (I_C - I_D) dV}{2A\nu\Delta V} \quad (S1)$$

where ΔV is the voltage window, I_C and I_D are charging and discharging currents respectively, A is the footprint area of the device including interfinger space and ν is the scan rate. The areal capacitance was also extracted from galvanostatic charge-discharge curves using Equation S2:

$$C_{A,GCD} = \frac{|I_D|\Delta t}{A\Delta V} \quad (S2)$$

where I_D is the discharging current and Δt is the time of discharging. The areal energy density E_D and areal power density P_D of the MSCs provided in the paper were calculated using Equations S3 and S4 respectively:

$$E_D = \frac{C_{A,CV}\Delta V^2}{2} \quad (S3)$$

$$P_D = \frac{E_D}{\Delta V/\nu} \quad (S4)$$

Besides the characterization presented in the main text, the devices were characterized with voltage window of 2 V. The CV curves at 25 and 150 °C exhibit rectangularity (Figure S5 a,b, Figure S6 a,b), indicating the electrical double-layer capacitive behavior of our MSCs when scanning at large voltage windows. However, GCD characterization indicates the difficulty in charging the devices up to 2V at 150°C with low current densities (Figure S6 c-e).

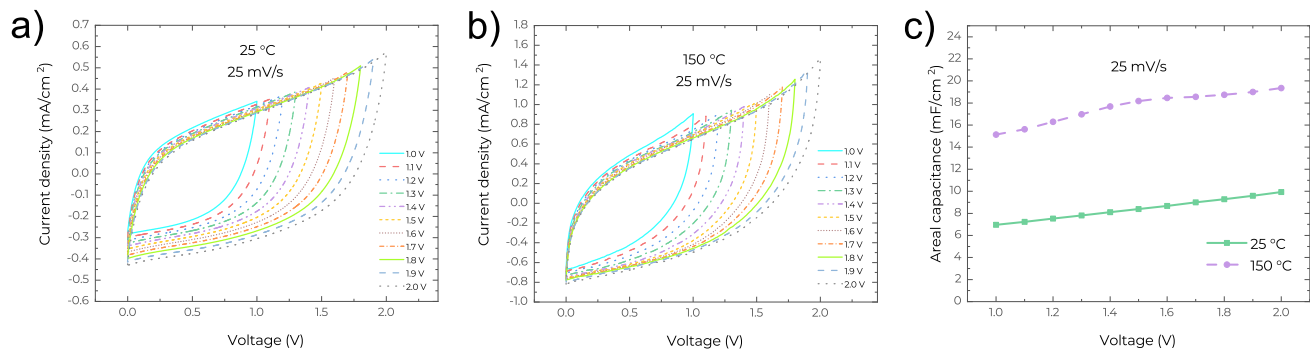


Figure S5 CV performance of the MSCs under wide voltage window up to 2.0 V. (a,b) CV curves at 25 mV/s under different voltage windows operating at (a) 25 °C and (b) 150 °C. (c) Areal capacitances extracted from the CV curves for different voltage windows operating at 25 °C and 150 °C.

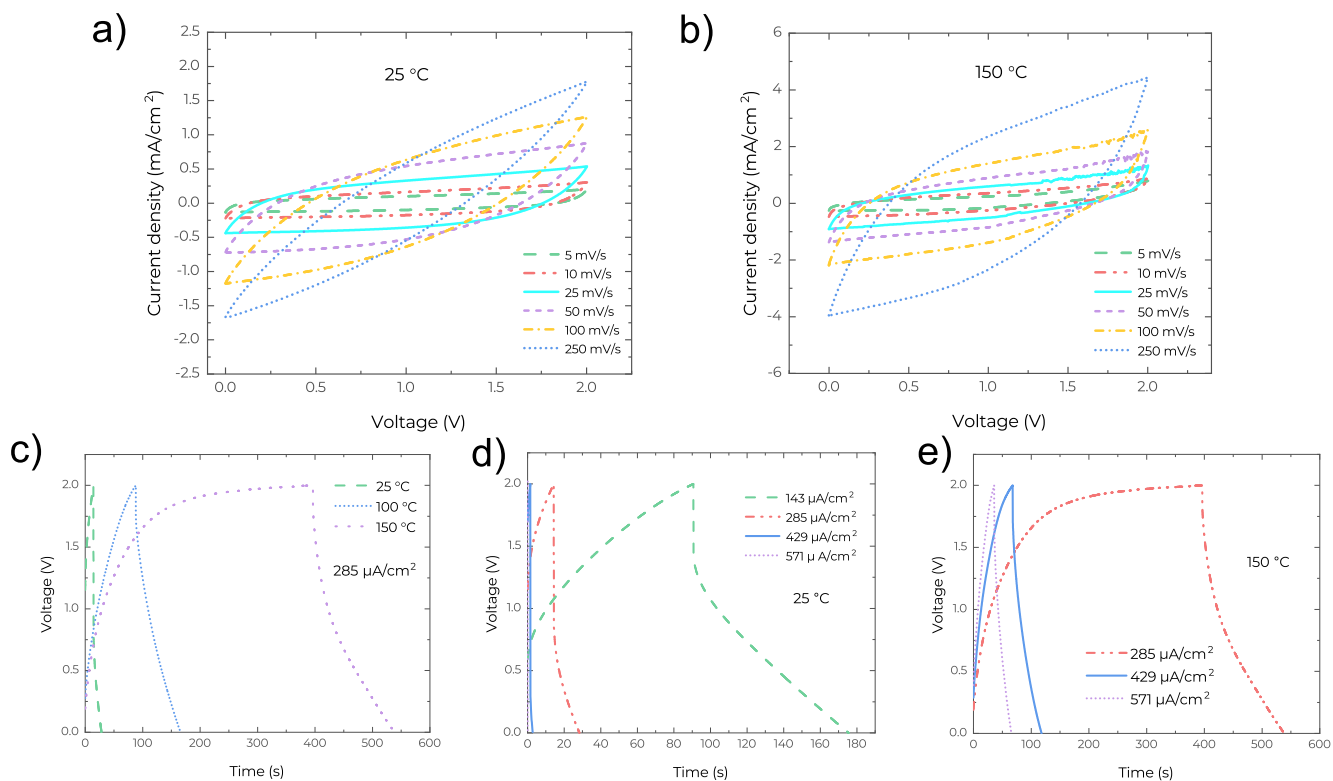


Figure S6 CV and GCD performance of the MSCs charged up to 2 V. (a, b) CV curves at different scan rates for the MSCs measured at (a) 25 °C and (b) 150 °C. (c) GCD curves measured under different temperatures at the same current density of 285 $\mu\text{A}/\text{cm}^2$. (d, e) GCD curves at different current densities operating under (d) 25 °C and (e) 150 °C.

References

- [1] V. Skrypnichuk, N. Boulanger, A. Nordenström and A. Talyzin, *The Journal of Physical Chemistry Letters*, 2020, **11**, 3032–3038.
- [2] A. Iakunkov, V. Skrypnichuk, A. Nordenström, E. A. Shilayeva, M. Korobov, M. Prodana, M. Enachescu, S. H. Larsson and A. V. Talyzin, *Phys. Chem. Chem. Phys.*, 2019, **21**, 17901–17912.

- [3] Shalu, S. K. Chaurasia, R. K. Singh and S. Chandra, *The Journal of Physical Chemistry B*, 2013, **117**, 897–906.